Computational and Structural Biotechnology Journal 18 (2020) 3368–3376

COMPUTATIONAL AND STRUCTURAL BIOTECHNOLOGY JOURNAL

journal homepage: www.elsevier.com/locate/csbj

Functional divergence of flagellar type III secretion system: A case study in a non-flagellated, predatory bacterium

Alex M. Fulano [a], Danyu Shen [a], En-Hui Zhang [a], Xi Shen [a], Shan-Ho Chou [b], Tohru Minamino [c], Gerardo Puopolo [d,e], Guoliang Qian [a,*]

[a] College of Plant Protection (Laboratory of Plant Immunity; Key Laboratory of Integrated Management of Crop Diseases and Pests), Nanjing Agricultural University, Nanjing 210095, PR China
[b] Institute of Biochemistry, and NCHU Agricultural Biotechnology Center, National Chung Hsing University, Taichung, Taiwan, ROC
[c] Graduate School of Frontier Biosciences, Osaka University, 1-3 Yamadaoka, Suita, Osaka 565-0871, Japan
[d] Department of Sustainable Agro-ecosystems and Bioresources, Research and Innovation Centre, Fondazione Edmund Mach, Via E. Mach 1, 38010 San Michele all'Adige, Italy
[e] Center Agriculture Food Environment (C3A), University of Trento, Via E. Mach 1, 38010 San Michele all'Adige, Italy

ARTICLE INFO

Article history:
Received 7 September 2020
Received in revised form 22 October 2020
Accepted 23 October 2020
Available online 10 November 2020

Keywords:
Flagellar type III secretion system
Non-flagellated bacteria
Lysobacter
Antifungal toxin

ABSTRACT

The lack of functional flagella and the ability to prey upon other microorganisms are well-known traits of *Lysobacter enzymogenes*, a plant beneficial bacterial species. Here, we report a possible link between these two traits in the model strain *L. enzymogenes* OH11 (OH11). The genome of OH11 encompasses several homologous genes involved in the flagellum formation but it lacks a functional *fliC*, encoding the flagellin. Despite the lack of the main component of the flagellum, OH11 genome includes genes involved in the flagellar type III secretion system (FT3SS), which is commonly deployed by flagellated bacteria to transport flagellar subunit proteins. To understand the role played by FT3SS in OH11, we showed that the remaining FT3SS genes were expressed under laboratory conditions. Subsequently, we showed that the identified FT3SS genes involved in the secretion of the hook-capping protein FlgD, suggesting OH11 likely possessed a functional FT3SS system. Blocking FT3SS in OH11 via inactivation of the ATPase FliI impaired the secretion of the proteins Le3970 (protease), Le4493 (ß-1,3-glucanase A) and Le1659 (halo acid dehalogenase family), that showed a toxic activity against the yeast *Saccharomyces cerevisiae*. The possible link between FT3SS and OH11 antagonism towards *S. cerevisiae* was also confirmed by loss of toxicity in both mutants of Δ*fliI* and Δ*flhB* that lacks the FT3SS structural gene *flhB* when co-cultured with the yeast strain. The design of synthetic proteins toxic against the Gram-negative bacterium *Ralstonia solanacearum* further supported the involvement of FT3SS in the ability of OH11 to parasitize other microorganisms. Overall, these results revealed a possible cooption of components of FT3SS system in the competition with other microorganisms in the plant beneficial bacterium OH11 and highlighted a functional divergence of FT3SS between flagellated and non-flagellated bacteria.

1. Introduction

Motile bacteria move toward or away from either favourable or unfavourable conditions, with the help of cell surface appendages (such as the flagellum), which play key roles in bacterial motility and adhesion process, biofilm formation, and virulence [1–4]. The flagellum structure is made up of an extracellular filament comprising the protein named flagellin connected to a basal body functioning as a rotary motor through a flexible hook [1]. Flagellar assembly is a rather complicated process involving many flagellar proteins, the export of which beyond the cellular membranes is dependent on its specific protein export apparatus, which shares similarities with type III secretion systems (T3SS) in pathogenic bacteria [5]. The flagellar type III secretion system (FT3SS), on the other hand, is composed of a proton motive force (PMF)-driven transmembrane export gate complex (comprising FlhA, FlhB, FliP, FliQ, and FliR) and a cytoplasmic ATPase ring complex (including FliH, FliI, and FliJ). The cooperation between the transmembrane export gate and the ATPase ring complex drives the transport of flagellin from the cytoplasm to the distal end of the growing flag-

* Corresponding author at: Nanjing Agricultural University, No. 1 Weigang, Nanjing City, Jiangsu Province 210095, China.
E-mail addresses: Shendanyu@njau.edu.cn (D. Shen), shchou@nchu.edu.tw (E.-H. Zhang), shchou@nchu.edu.tw (S.-H. Chou), tohru@fbs.osaka-u.ac.jp (T. Minamino), gerardo.puopolo@unitn.it (G. Puopolo), glqian@njau.edu.cn (G. Qian).

https://doi.org/10.1016/j.csbj.2020.10.029
2001-0370/

ellar structure [5–8]. Although FT3SS seems to be related mainly to flagellum formation on the bacterial cell surface, its component homologs are also found in bacteria that contains no functional flagella, such as the endomutualistic bacterium *Buchnera aphidicola* [9]. In this non-flagellated bacterial species, the FT3SS genes are proposed to serve diverged roles, but no functional study has been done [9].

Most of the bacterial species belonging to the genus *Lysobacter* are also non-flagellated [10]. These bacteria are common inhabitants of agricultural soils and they are characterized by the ability to prey other microorganisms through production of antibiotics and lytic enzymes [11–13]. Among them, the model strain *L. enzymogenes* OH11 (OH11) is a proficient predator of fungi through the secretion of a huge set of extracellular lytic enzymes [14].

Recently, we showed that OH11 genome has homologous FT3SS components despite lacking a functional flagellum [15]. Since it has been shown that this non-flagellated bacterial strain moves on solid surfaces using type IV pili (T4P) [16,17], it is possible that FT3SS-related genes have adapted to exert other functions. Indeed, we found that several FT3SS components (FlhA, FlhB, FliI and FliR) in OH11 have acquired a distinct function to control T4P-driven twitching motility [15]. Here, by using the parasitic interaction between OH11 and the model fungus *Saccharomyces cerevisiae* as a working system, we provided evidence suggesting that the non-flagellated OH11 employs the FT3SS system to secrete non-flagellar proteins toxic to *S. cerevisiae*, and further to inhibit the growth of *S. cerevisiae*. Based on these novel insights into FT3SS, we developed a strategy to allow the wild-type OH11 to export heterologous antibacterial toxins in a FT3SS-dependent manner, thereby enabling this bacterium to gain an additional antibacterial activity. Thus, this is the first report describing that the FT3SS has diverged to mediate the antagonistic interaction among a non-flagellated environmental bacterium and fungus as well as bacterial pathogens.

2. Materials and methods

2.1. Bacterial strains, plasmids and culture conditions

The bacterial strains and plasmids used in this study are listed in supplemental Table S1. The cloning host, *Escherichia coli* DH5α grown at 37 °C in Luria Broth (LB) was used during recombinant plasmid generation. LB was amended with 25 μg/mL gentamicin (Gm) and 100 μg/mL X-gal (5-bromo-4-chloro-3-indolyl-beta-d-galactopyranoside) for culturing *E. coli* DH5α recombinant strains. *E. coli* strain BL21 (DE3) was used as the host for the expression FliI-His/$FliI_{Xoo}$-His fusion proteins. Generally, OH11 wild-type and mutants were grown in 20 mL LB medium at 28 °C. LB medium supplemented with final concentrations ranging from 25 to 150 μg/mL of kanamycin (Km) and Gm was used when required.

2.2. Bioinformatics analyses

The flagellum biogenesis proteins retrieved from the genome of the phylogenetically related bacterial strain *Xanthomonas oryzae* pv. *oryzae* (*Xoo*) PXO99A (NC_010717.2) were used as queries to run local BLASTp to identify the respective homologs in the OH11 genome. A protein was considered present when the E-value was lower than 10^{-5} and a percentage of similarity with the corresponding *Xoo* homologous protein was higher than 40%.

2.3. Genetic methods

In-frame deletion mutant of *flhA*, *flhB*, *fliP*, *fliI*, *fliQ* or *fliR* in OH11 was generated in a previous work [15] and stored at length at −80 °C. Construction of the complementation or overexpression plasmids was carried out as described earlier [18]. Briefly, the DNA fragment containing the full-length gene and its predicted promoter region was amplified by PCR with different primer pairs (Table S2) and cloned into the broad-host vector pBBR1-MCS5 (Table S1). Further, each of the construct was transformed into the wild-type OH11 and its derivative mutants by electroporation and the resulting transformants were selected on the LB agar containing both Km and Gm. For heterologous gene complementation, the plasmid pBBR1-MCS5 was cloned with each intact fragment of certain FT3SS genes (fused with a Flag tag) of *Xoo* PX099A (GenBank accession no. NC_010717.2) (Table S1). The resulting plasmids were transformed into respective competent cells of in-frame deletion mutants of OH11 by electroporation. The resulting clones were screened by colony PCR and further validated by sequencing.

2.4. Protein expression, purification, and ATPase activity assay

For detection of expression of FT3SS proteins in OH11, Western blotting assays were carried out according to previous work [19]. Briefly, cells of test strains were collected as already stated and frozen at −80 °C. Bacterial cells were disrupted to obtain lysates of soluble proteins. The soluble proteins were separated by sodium dodecyl sulphate–polyacrylamide gel electrophoresis (SDS-PAGE) and immobilized onto a PVDF membrane. The homologous FT3SS proteins were then probed by specific polyclonal anti-antibodies with a dilution of 1/20,000 (generously provided by Prof. Tohru Minamino). Secondary antibody, HRP-conjugated anti-rabbit secondary antibody (Abmart, Shanghai, China), was used at 1/20,000.

For protein expression in *E. coli*, the coding region of the FliI homolog (MN626605) of wild-type OH11 and flagellar $FliI_{Xoo}$ (PXO_06165) were amplified by PCR using the genomic DNA of the respective bacterial strain as a template. Each purified PCR product was digested and ligated into equally digested expression vector pET30(a) and subsequently transformed into *E. coli* BL21 (DE3). The transformed *E. coli* BL21 strains were grown at 37 °C in a rotary shaker (200 rpm) to a final optical density at 600 nm (OD_{600}) of 0.5, followed by supplementation of isopropyl β-D-1-thiogalactopyranoside (IPTG), and further incubated at 28 °C for six hours. The transformed *E. coli* BL21 cells were pelleted by centrifugation (5000 rpm, 4 °C, and 10 min) and re-suspended in lysis buffer [phosphate-buffered saline (1 × PBS), 10 mM phenylmethylsulfonyl fluoride (PMSF), and protease inhibitor]. Lysis was carried out by sonication, and the resultant suspensions were then centrifuged (13,000 rpm, 4 °C, 30 min) to obtain the soluble extract. The two proteins were further individually purified using the Ni2-resin (GE Health, Shanghai, China). The mixtures of soluble extracts and pre-equilibrated Ni2-resin were incubated at 4 °C for one hour. The columns containing the resin with bound FliI-His or $FliI_{Xoo}$-His fusion protein were washed extensively with re-suspension buffer (50 mM PBS, 30 mM imidazole, and 300 mM NaCl). The resulting protein was eluted and concentrated using 250-mM imidazole by ultrafiltration centrifugal tube (Millipore UFC501096) and centrifugation (10,000 rpm, 4 °C, and 20 min), respectively. The purified FliI-His was subjected to SDS-PAGE for validation before determining its ATPase activity.

ATPase activity assay was carried out as previously described [20]. Briefly, the ATPase activity was quantified by subjecting the respective absorbance of purified proteins to the calibrated equation of phosphate standard from the standard curve. Reaction mixtures comprised various 1:1 serial dilution of purified ATPases, 4 mM ATP, 100 mM Tris-HCl, and 4 mM $MgCl_2$. The reaction mixtures were then left on the bench at room temperature for 25 min.

To check ATP degradation or phosphate contamination, we included a control mixture without protein. Each reaction mixture was in triplicate, with data recorded by measuring optical density at 640 nm (OD_{640}). To obtain OD_{640} values, we further subtracted OD_{640} values of the ATP without protein (ATP degradation or phosphate contamination) at each ATP concentration. To determine released phosphate from protein samples, we followed the instructions of the kit (BIOMOL GREEN, Farmingdale, NY, USA) by comparing protein sample absorbance with a phosphate standard curve.

2.5. Identification of secreted proteins and protein secretion assay

Wild-type OH11 and its derivative strains were grown at 28 °C in 1/10 TSB until OD_{600} reached 1.5. Total secreted proteins from bacterial cultures were obtained as described previously [21] with a slight modification. Briefly, 40 mL of each culture sample was subjected to centrifugation (6000 rpm, 4 °C, and 30 min) to separate supernatants from whole cells. Supernatant fractions were filtered using 0.22-μm Millipore under ice-cold conditions. Next, 10% (v/v) trichloroacetic acid (TCA) was added to the filtered supernatants and stored at 4 °C overnight to allow the precipitation of all secreted proteins. The resulting precipitates were pelleted by centrifugation (12,000 rpm, 4 °C, and 30 min), and subsequently washed in ice-cold acetone three times. The harvested precipitates were further re-suspended in ice-cold sterile distilled water (1 mL) before subjecting them to centrifugation (12,000 rpm, 4 °C, and 15 min). While whole bacterial cells were suspended in 60 μL 2 × SDS buffer, the precipitates were suspended in 100 μL 1 × SDS buffer before adding SDS-PAGE loading buffer. Both precipitates and cellular samples were subjected to SDS-PAGE. Four gel bands (LE-1, LE-2, LE-3, and LE-4) invisible in the precipitates of the *fliI* mutant, but present in the wild-type OH11 and *fliI* complemented strains, were excised and subjected to liquid chromatography connected with tandem mass spectrometry (LC-MS-MS) (BGI company, Beijing, China) for protein identification. In brief, each gel band was cleaned several times by the cleaning solution containing 50% acetonitrile and 25 mM ammonium bicarbonate to completely remove the coomassie blue. Then 10 mM dithiothreitol was added and incubated at 56 °C for 1 h, followed by supplement of 55 mM iodoacetamide for 45 min at room temperature with dark. After enzymatic digestion at 37 °C for 4 h [trypsin enzyme (μg): substrate protein (μg) = 1: 20], the digested peptides were subjected into mass spectrometry (Q-Exactive HF, Thermo Fisher Scientific) to obtain the mass spectrum of the proteins in these gels. The mass spectrum was searched in the genome of strain OH11 (accession number: GCA_003789105.1) to match the respective protein with minimum of 1 unique peptide. The false discovery rate (FDR) was set to 1% at peptide spectra match (PSM) level. For protein secretion assay, the coding region of each selected protein fused with a Flag tag was cloned into pBBR1-MCS5, provided with a native promoter capable of driving transcription of each test gene cloned downstream (Table S1). Each final construct was individually introduced into wild-type OH11 and the Δ*fliI* strain. Precipitates of secreted proteins were prepared in detail as described above. The collected precipitates were first dissolved and separated by SDS-PAGE and immobilized onto a PVDF membrane. The well-characterized transcription factor Clp [19] of OH11 was used as an intracellular protein control. Monoclonal antibody specific for the Flag tag primary antibody (Abmart, Shanghai, China) was applied at 1/5000 titer followed by detection with an HRP-conjugated anti-mouse secondary antibody at the same concentration. Clp was probed by a specific polyclonal anti-antibody with a dilution of 1/20,000 [19]. Secondary antibody, HRP-conjugated anti-rabbit secondary antibody (Abmart, Shanghai, China), was used at 1/20,000.

2.6. Identification of FT3SS-controlled secreted proteins with potential for fungicidal or bactericidal activity

Expression of the *Xanthomonas* and *Pseudomonas* virulence-associated type III secretion (T3SS) effectors in yeast cell is proved to be a powerful approach to identify the target bacterial effectors that affect yeast cell growth and viability [22,23]. We applied such an approach to investigate whether the FT3SS-controlled secreted proteins identified in OH11 are toxic to yeast cell, because FT3SS and the virulence-associated T3SS have similar architecture [5]. To carry out the assay using *E. coli* DH5α, the constructs expressing full-length of each OH11 gene of interest (GOI) were cloned into the vector pBAD/Myc-His B (Table S1) and transformed into *E. coli* DH5α. Then, the transformed strains were grown in LB plates for 12 h. Subsequently, 2 μL of cell cultures were serially diluted and spotted in triplicate onto fresh LB plates with or without 0.1% arabinose. The plates were incubated at 37 °C for 48 h before photo-taking.

In the case of assays using the yeast, *S. cerevisiae* W303, each selected FT3SS-controlled secreted protein gene was cloned into pSB157 (Table S1), in which the target gene transcription was driven by galactose-inducible promoter [24]. Subsequently, each construct was transformed into *S. cerevisiae* W303 using lithium acetate (LiAc)-mediated yeast transformation, as described previously [25]. Individual yeast cultures harboring recombinant plasmids were serially diluted and plated onto 2% glucose medium in triplicates. The same serially diluted yeast cultures were plated onto 2% galactose medium in triplicate. The yeast cultures were incubated at 28 °C for 48 h before photo-taking.

To identify FT3SS-controlled secreted protein(s) with potential for bactericidal activity, we carry out the assay using *E. coli* DH5α. The constructs expressing full-length of each selected FT3SS-controlled secreted protein gene was cloned into the vector pBAD/Myc-His B (Table S1), in which the target gene transcription was driven by arabinose. The resultant constructs were transformed into *E. coli* DH5α. Then, the transformed strains were grown in LB plates for 12 h. Subsequently, 2 μL of cell cultures were serially diluted and spotted in triplicate onto fresh LB plates with or without 0.1% arabinose. The plates were incubated at 37 °C for 48 h before photo-taking.

As a reference control, *avrRx01* (AEQ98135), encoding the virulence-associated T3SS effector protein with known antibacterial and anti-yeast activities [23,26], from *X. oryzae* pv. *oryzicola* (*Xoor*) BLS256 was cloned into *E. coli* DH5α and *S. cerevisiae* W303. In each assay, three replicates were used for each treatment and experiments were repeated three times.

2.7. Colorimetric yeast killing assay

Cells of *S. cerevisiae* AH109, a LacZ-labelled strain that acquires a blue colour when grown in the presence of X-gal, were grown in yeast extract peptone (YPD) overnight at 30 °C before re-culturing them in fresh YPD and growing until OD_{600} reached 1.0. Wild-type OH11 and its derivatives were grown under laboratory conditions as stated before for overnight. The strains were transferred to fresh LB and allowed to grow until OD_{600} reached 1.0. Yeast and bacterial cells were individually washed in YPD and co-cultured by spotting them onto YPD agar at different ratios. The co-cultures were then incubated at 28 °C and photographed after 48 h interaction, with the experiment repeated three times.

2.8. Heterologous expression of recombinant antibacterial toxins and antibacterial assay

The fusion of heterologous gene fragments was carried out as described previously [27,28]. As the N-terminal flagellin (FliC) seg-

ment from *Salmonella* can act as a FT3SS signal to facilitate the export of heterologous proteins, we thus applied such a strategy with slight modifications. In brief, a 399-bp DNA fragment of $fliC_{Xoo}$ containing its predicted N-terminal signal segment was amplified and fused with the synthetic peptides AsR498 (12 aa) and AspR117 (34 aa) produced in plant garlic (*Allium sativum*). Both AsR498 and AspR117 are characterizedwith antibacterial activity [29]. The sequence of AsR498 and AsR117 and primers used in this assay were listed in Table S2. The resultant fragments, designated as $FliC^{N133}_{Xoo}$-AsR498 and $FliC^{N133}_{Xoo}$-AsR117, respectively, were individually fused with a C-terminal Flag tag and cloned into the broad-host vector pBBR1-MCS5. Transcription of $FliC^{N133}_{Xoo}$-AsR498 and $FliC^{N133}_{Xoo}$-AsR117 was driven by a constitutive expression promoter (the promoter of gentamicin resistance gene) in the plasmid. Each final construct was individually introduced into wild-type OH11 or *fliI* mutant. The secreted and cellular profiles of the recombinant proteins were determined by Western blotting using anti-Flag antibody as descried above.

Antibacterial assay of OH11 derivatives against *Ralstonia solanacearum* GMI1000 (Table S1) was carried out as described previously [29] with slight modifications. In brief, the indicator bacterial stain *R. solanacearum* GMI1000 was grown in Nutrient Broth medium at 28 °C to an OD_{600} 1.5. Subsequently, 400 μL of indicator bacterial cells were mixed with 4 mL of semi-solid (0.3% agar) Nutrient Agar (NA) and used to make a lawn on the normal NA agar (1.8%) plates. Cells of all OH11 derivative strains grown in LB medium at 28 °C till OD_{600} 1.5 were collected and washed three times by fresh LB to get rid of antibiotics. The concentration of bacterial suspensions was standardized to an OD_{600} of 1.0. For each bacterial suspension sample, 7.5 μL aliquot were spot inoculated on the indicator bacterial lawn. The occurrence of an inhibition zone surrounding the developed macrocolonies (antibacterial activity) was monitored after 36 h incubation at 28 °C.

Each treatment included three replicates (spotted macrocolonies) and three independent experiments were carried out.

3. Results

3.1. The non-flagellated Lysobacter enzymogenes OH11 is provided with a functional FT3SS-like system

The bioinformatics analysis allowed to determine the presence of flagellar genes in OH11 such as the flagellar hook gene (*flgE*), basal-body rod genes (*flgC* and *flgG*), L-ring gene (*flgH*), P-ring gene (*flgI*), MS-ring gene (*fliF*), C-ring gene (*fliN*), and hook cap gene (*flgD*) (Fig. 1A, 1B and Table S3). However, quite a few of flagellar assembly genes are missing (Fig. 1A, 1B), as the case of *fliC* responsible for the flagellin formation.

Five genes, namely *flhA*, *flhB*, *fliP*, *fliQ*, and *fliR*, whose products form the PMF-driven export gate complex of FT3SS inside the basal body MS ring, were detected in OH11 genome using all flagellar components from the phylogenetically closely-related *Xoo* PXO99A as queries (Fig. 1A, B and Table S3). Interestingly, the OH11 genome lacks genes encoding FliH and FliI whereas encompasses *fliI*, encoding of the export apparatus (Fig. 1A, B and Table S3). In agreement with gene predictions and our earlier finding that several FT3SS genes (*flhA*, *flhB*, *fliI* and *fliR*) are required for the *L. enzymogenes* twitching motility [15], we showed that introduction of plasmids containing each canonical FT3SS gene counterpart from *Xoo* PXO99A restored the deficiency of the OH11 *flhA*, *flhB*, *fliI* or *fliR* mutant in producing twitching motility (Fig. S1), supporting our notion that the identified FT3SS-like genes most likely belong to the core of FT3SS machine.

Subsequently, we created in-frame deletion mutants for *flhA*, *flhB*, *fliI*, *fliP*, *fliQ*, and *fliR* to investigate the role played by FT3SS-like system in OH11 behavior. Their corresponding gene products (FlhA, FlhB, FliI, FliP, FliO, and FliR) were detected in the wild-type OH11, but not in its derivatives by immunoblotting (Fig. 1C). These results indicated that the six FT3SS proteins are expressed in OH11 under the controlled experimental conditions. We then explored whether the FT3SS-like genes could assemble a functional export system in OH11. To do that, we randomly selected FlgD as a candidate. The FlgD-Flag fusion was constructed and introduced into the wild-type OH11 and its derivatives, followed by immunoblotting using an anti-Flag antibody. At OD_{600} 1.5, the FlgD-Flag fusion was detected in the wild-type OH11 supernatant, but not in either Δ*flhA*, Δ*flhB*, Δ*fliI*, Δ*fliP*, Δ*fliO*, or Δ*fliR* mutant, in which this fusion protein was found in the cytoplasm only (Fig. 1D).

3.2. FT3SS in Lysobacter enzymogenes OH11 contributes to the inhibition of Saccharomyces cerevisiae cell growth by promoting the export of antifungal toxins

As FliI is a well-known FT3SS-specific ATPase required for the export of flagellar subunit proteins in flagellated bacteria, we focused our analysis on OH11 *fliI* mutant derivative to better determine its role in OH11. Firstly, we found that the OH11 FliI-His fusion protein exhibited an ATPase activity similar to the $FliI_{Xoo}$-His tag protein deriving from the flagellated *Xoo* PXO99A, used as a reference (Fig. 2A). Using comparative SDS-PAGE assays, we found that four putative proteins ranging from 15 to 40 kDa were present in the profile of the secreted proteins of the wild-type OH11 and Δ*fliI* complemented strains whereas they were missing in the Δ*fliI* strain (Fig. 2B). In contrast, no differences were found in the proteins ranging from 15 to 40 kDa present in the cytoplasm of OH11 and its derivatives (Fig. 2B). Among the OH11 wild-type specific bands, nine proteins were identified by LC-MS-MS analysis. According to their functional annotations, none of these proteins were predicted to be involved in the flagellum formation process (Fig. 2C), indicating that the FliI-mediated FT3SS-like system in OH11 is likely to mediate the secretion of non-flagellar proteins also.

Five corresponding genes of the secreted proteins (Fig. 2C) were randomly selected, cloned and transferred into the wild-type OH11 and its *fliI* mutant derivative to confirm this finding. The gene *clp*, encoding a cytoplasmic transcriptional factor [19], was also included as an internal control to reduce the possibility that the presence of selected proteins in the culture medium was a consequence of cell lysis. The analysis of the protein secretion revealed that, similarly to Clp, the selected proteins were present in the cytoplasm in both wild-type OH11 and Δ*fliI*. In contrast, the selected proteins were found in the extracellular fraction only in the case of wild-type OH11 (Fig. 2D).

To determine whether the secreted proteins would participate in the antagonistic interaction between OH11 and fungi, the corresponding OH11 genes of four selected secreted proteins (Fig. 2C) were cloned in *S. cerevisiae* W303 and *E. coli* DH5α to test their toxic effect. Similar to the reference control *avrRx01* [23,26] from *Xoor* BLS256, the expression of OH11 genes encoding ß-1-3-glucanase (MN626614), protease (MN626612) and hydrolase (MN626617) belonging to the halo acid dehalogenase (HAD) family in the *S. cerevisiae* W303, resulted the inhibition of yeast growth (Fig. 3A). Among the selected OH11 genes, the expression of the gene Le3234 (MN626613), encoding an outer membrane protein, did not show any toxic effect against *S. cerevisiae* W303 (Fig. 3A). Differently from the reference control *avrRx01*, the expression of all selected genes did not show any toxic effect against *E. coli* DH5α (Fig. 3B).

To confirm the above findings, we carried out an additional inhibition assay using *S. cerevisiae* AH109, a LacZ-labelled yeast

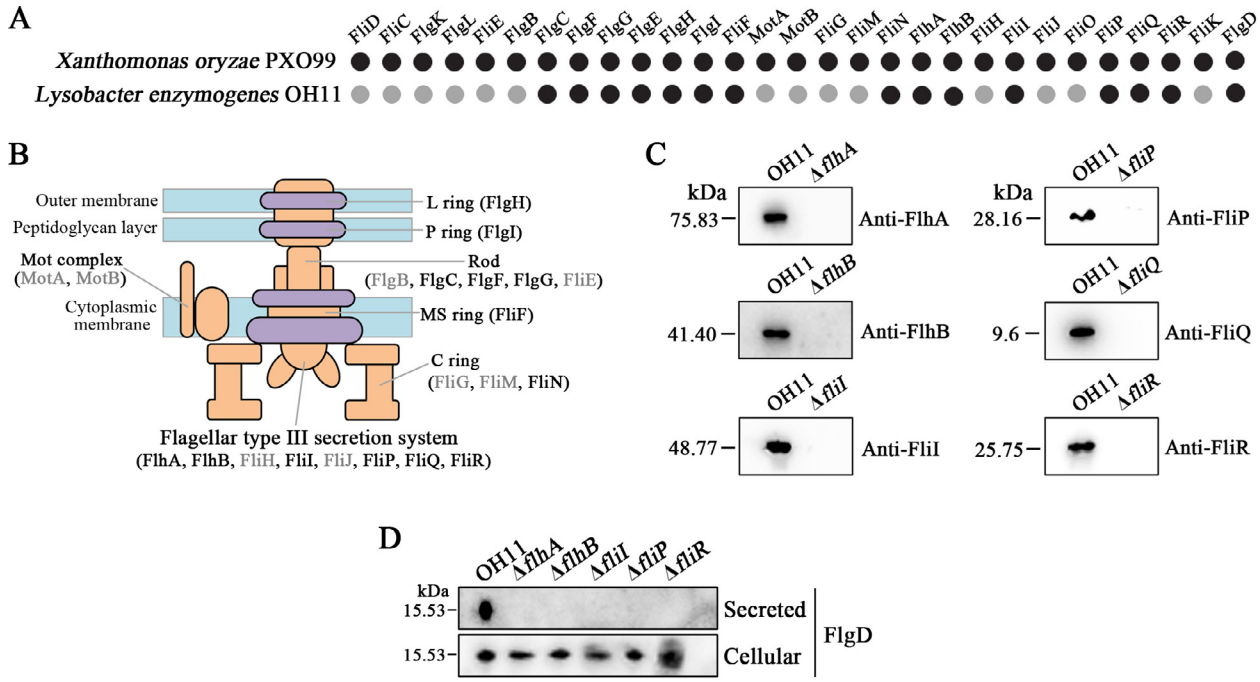

Fig. 1. The non-flagellated *Lysobacter enzymogenes* OH11 likely encoded a FT3SS-like system that could mediate the export of its flagellar proteins. (A) *Lysobacter enzymogenes* OH11 (OH11) genome includes several flagellum-assembly gene homologs. Protein sequences of flagellar proteins of *Xanthomonas oryzae* pv. *oryzae* PXO99 (dark dots) were used as queries in a BLASTp analysis. The presence and absence of the flagellar assembly genes in OH11 genome are indicated by filled black circles and filled gray circles, respectively. Details in Table S3. **(B)** A schematic diagram of the basal body structure of FT3SS. Genes with gray indicate their absence in the genome of OH11, as described in Fig. 1A. **(C)** Expression of the FT3SS components in OH11. Western blotting analyses of cellular expression of the FT3SS genes in OH11 and its derivatives. Strains were cultivated in 1/10 TSB and cells were collected when OD_{600} reached 1.5. Cellular abundance of each FT3SS component (FlhA, FlhB, FliI, FliP, FliQ or FliR) was detected in wild-type OH11, but not in their respective in-frame deletion mutants (Δ*flhA*, Δ*fllhB*, Δ*fliI*, Δ*fliP*, Δ*fliQ*, or Δ*fliR*) by using specific polyclonal antibodies. **(D)** Secretion of the retained flagellar assembly protein FlgD is dependent on the presence of FT3SS in OH11. Gene encoding FlgD was fused with a Flag-tag and introduced into the wild-type OH11 and individual FT3SS-defective mutant (Δ*flhA*, Δ*fllhB*, Δ*fliI*, Δ*fliP*, Δ*fliQ*, or Δ*fliR*). Signal of the respective fusion protein was detected in the culture supernatant (defined as "Secreted") of wild-type OH11 but not the FT3SS-defective mutants. In contrast, its presence in the cytoplasm (defined as "Cellular") was observed in both wild type and the FT3SS-defective mutants.

strain, as a prey. After co-incubation at ratios of 1:1 and 5:1 for 48 h, the wild-type OH11 visually reduced the survival of *S. cerevisiae* AH109, while both mutants of Δ*fliI* and Δ*flhB* that lacks the FT3SS structural gene *flhB* failed to kill *S. cerevisiae* AH109 at either ratio of 1:1 or 5:1 (Fig. 3C).

3.3. Involvement of Lysobacter enzymogenes OH11 FT3SS in the export of recombinant peptides toxic against Ralstonia solanacearum

On the basis of the achieved results, we designed two recombinant toxins active against Gram-negative bacteria. A 133-amino-acid portion of the N-terminal sequence (referred as $FliC_{Xoo}^{N133}$) of $FliC_{Xoo}$ comprising a predicted flagellin signal was fused with two individual synthetic peptides (AsR498 and AsR117) with known antibacterial activity from garlic [29], resulting in two recombinant antimicrobial toxins, namely $FliC_{Xoo}^{N133}$-AsR498-Flag and $FliC_{Xoo}^{N133}$-AsR417-Flag (Fig. 4A). Next, the wild-type OH11 and the Δ*fliI* strains served as hosts to evaluate the secretion of the recombinant toxins. As shown in Fig. 4B, both recombinant toxins were observed in the culture supernatant of the wild-type OH11, but not in that of the Δ*fliI* (Fig. 4B). Accordingly, the wild-type OH11 harboring either recombinant toxins inhibited the growth of *R. solanacearum* GMI1000, while the wild-type OH11 carrying the full-length $FliC_{Xoo}$ or its truncated $FliC_{Xoo}^{N133}$ did not display such an inhibitory effect (Fig. 4C). Similarly, no toxic activity against *R. solanacearum* GMI1000 was observed when plasmids where transferred in Δ*fliI* (Fig. 4C), confirming its potential involvement in the secretion of antimicrobial toxins involved in the interaction with other microbes.

4. Discussion

At the establishment of the genus, *Lysobacter enzymogenes* species was reported as nonmotile due to the lack of flagella [11]. With extensive research carried out in these years, we became aware that members of this bacterial species move in the environment using type IV pili [17]. Moreover, the comparison of the genomes of bacterial strains belonging to *L. antibioticus*, *L. capsici*, *L. gummosus*, and *L. enzymogenes* revealed that these species are provided with the genes responsible for the formation of a not functional flagellum [30]. These findings prompted us to investigate the role played by genes involved in the formation of the not functional flagellum in the behavior of OH11.

In this study, the genome mining analysis revealed that, OH11 genome is provided with most of the genes involved in flagellum formation similarly to the *Lysobacter* spp. strains analyzed by De Bruijn et al. [30]. Moreover, the absence of *fliC* gene, encoding the flagellin, might explain why OH11 lacks a surface-attached flagellum. As flagellar filament proteins can potentially act as antigenic inducers of host immune responses [30–32], it is tempting to hypothesize that the lack of these genes in *L. enzymogenes* species might be a result of an evolved mechanism for this plant beneficial bacterium to evade host detection. Despite the lack of *fliC*, OH11 genome encompasses most of the genes encoding the components of the FT3SS involved in flagellin export. Genes encoding FliH and FliJ, components of a cytoplasmic ATPase ring complex that drives the export of flagellar subunit proteins via ATP hydrolysis in flagellated bacteria [5–7] were the only genes missing. Moreover, besides *fliN*, genes encoding FliG and FliM, components of the C

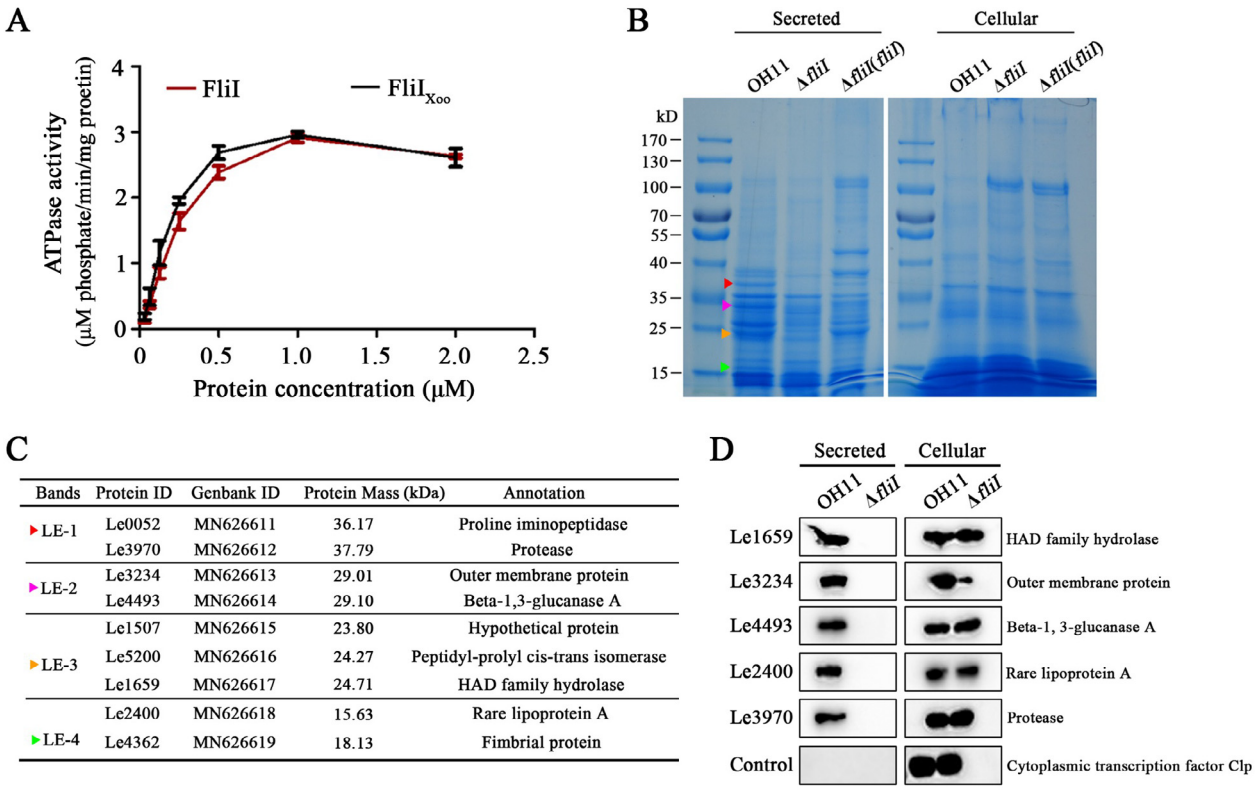

Bands	Protein ID	Genbank ID	Protein Mass (kDa)	Annotation
LE-1	Le0052	MN626611	36.17	Proline iminopeptidase
	Le3970	MN626612	37.79	Protease
LE-2	Le3234	MN626613	29.01	Outer membrane protein
	Le4493	MN626614	29.10	Beta-1,3-glucanase A
LE-3	Le1507	MN626615	23.80	Hypothetical protein
	Le5200	MN626616	24.27	Peptidyl-prolyl cis-trans isomerase
	Le1659	MN626617	24.71	HAD family hydrolase
LE-4	Le2400	MN626618	15.63	Rare lipoprotein A
	Le4362	MN626619	18.13	Fimbrial protein

Fig. 2. The flagellar FliI homolog modulated the secretion of several non-flagellar proteins in *Lysobacter enzymogenes* OH11. (A) ATPase activity of the *Lysobacter enzymogenes* OH11 (OH11) FliI (red line) and FliI$_{Xoo}$ (dark line) from *Xanthomonas oryzae* pv. *oryzae* PXO99A, a flagellated bacterium phylogenetically close to *Lysobacter* spp., used as a reference control. **(B)** SDS-PAGE analysis of total secreted and cellular proteins from wild-type OH11 and its derivatives at OD_{600} 1.5. Triangles with different colors indicated the gel bands missing in the *fliI* mutant (Δ*fliI*) but retained in wild-type OH11 and the complemented strain, Δ*fliI*(*fliI*). **(C)** Protein identification corresponding to the four selected gel bands indicated by color triangles in Fig. 2B using LC-MS-MS. **(D)** Western blotting validation of the five secreted proteins in a FliI-dependent manner in wild-type OH11. Genes encoding each test protein were individually fused with a Flag-tag and introduced into the wild-type and Δ*fliI* strain. Signal of each fusion protein was detected in the culture supernatant (defined as Secreted) of wild-type OH11, but not of the *fliI* mutant, while the cellular presence (defined as Cellular) was observed in both the wild type and Δ*fliI* strain. The cytoplasmic transcription factor Clp (25 kDa) was chosen as a control to show its absence in the cultural supernatant of the wild-type OH11 or Δ*fliI* strain. The assays were repeated three times with similar results. (For interpretation of the references to color in this figure legend, the reader is referred to the web version of this article.)

ring of the flagellar basal body were also not searched. However, we still could not rule out that *fliH*, *fliJ*, *fliG* and *fliM* homologues may be present in OH11 genome, but their sequence similarities with homologous genes from *Xoo* PXO99A, used as queries, are too low to be clearly identified.

Based on this evidence, we inquired about the reason why the non-flagellated OH11 maintained genes associated with FT3SS formation in its genome. Results achieved in this work revealed that OH11 appears to employ its FT3SS genes to assemble a functional FT3SS system involved in the secretion of the natively remaining flagellar proteins, such as FlgD. These new findings are consistent with our earlier observation that OH11 could transport the heterologous flagellin, FliC$_{Xoo}$ in a FT3SS-dependent manner, which is a canonical function of FT3SS in flagellated bacteria [5,15]. Since the secretion of FlgD into the culture media obviously depends on an intact basal body structure in the flagellated *Salmonella* strain [33], we might assume that the non-flagellated OH11 cells might be provided with a hook-basal body.

However, our results also unveiled the involvement of FT3SS in the OH11 ability to prey upon other microorganisms, another trait that characterizes the members of *L. enzymogenes* species. Indeed, the inactivation of the enzymatically active ATPase FliI blocked FT3SS functions in OH11 and, as a consequence, impaired the release of several non-flagellar proteins that showed a toxic effect on *S. cerevisiae* strains. This is also in agreement with recent works that highlighted the involvement of FT3SS in bacterial physiological processes other than flagellum formation. For instance, in the flagellated Gram-positive *Bacillus subtilis*, the FT3SS gene products were shown to facilitate the formation of flagellum-independent nanotubes that participate in cell–cell exchange of proteins or plasmids [34]. In the flagellated Gram-negative *Vibrio cholerae*, a deletion of the *flaA* encoding for the flagellin could trigger flagellum-dependent biofilm formation, which links the downstream intracellular signaling transduction pathway of c-di-GMP, a ubiquitous bacterial second messenger [35]. Moreover, we recently showed that several homologous components of FT3SS have acquired a novel function in the non-flagellated OH11 by modulating its ability to move on surface through twitching motility [15].

Plant associated bacteria possess multiple weapons to fend off microbial competitors. Currently, we know that type VI secretion system (T6SS) is an extensively-documented contact-dependent system that bacteria use to kill and lyse competing bacteria via translocation of toxic effector protein [36,37]. In addition, *Stenotrophomonas maltophilia* and *Xanthomonas citri* use type IV secretion system (T4SS) instead of T6SS to execute a similar function [38]. Both T6SS- and T4SS-dependent effector secretions are energy-costing processes, and require the presence of specific ATPases, such as ClpV in T6SS, and VirD4, VirB4, and VirB11 in T4SS [25,38]. In the present study, we provided experimental evidence showing that the FT3SS-like system in OH11 played key roles for the release of several antifungal toxins to establish the phenotype

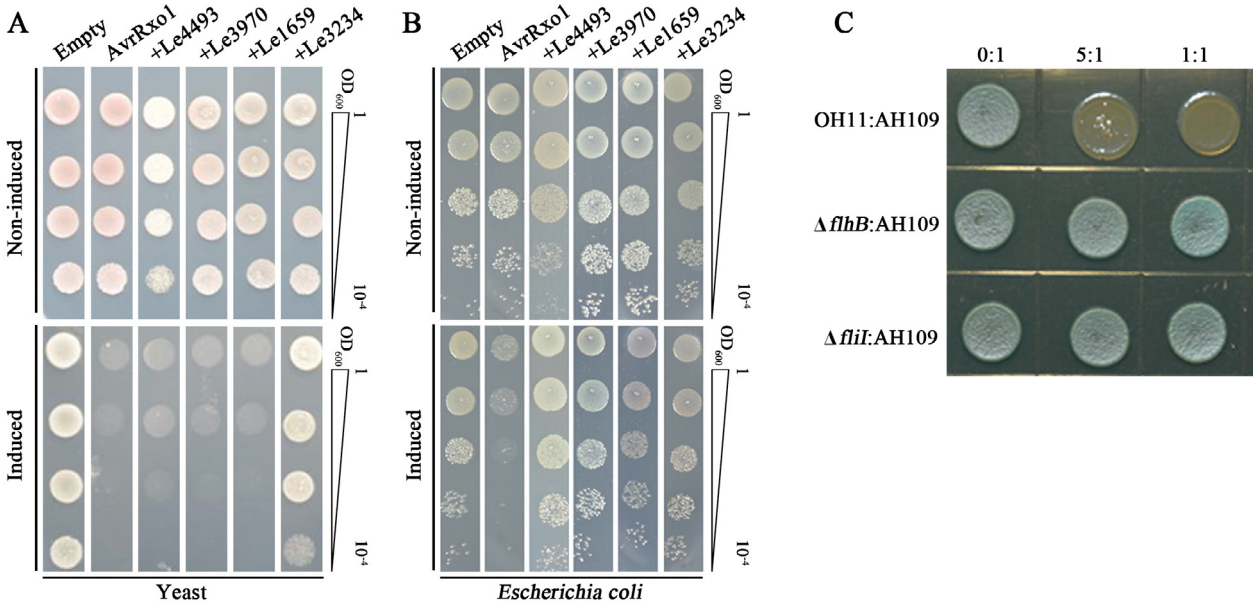

Fig. 3. The flagellar FliI homolog mediated the antagonistic interaction between the *Lysobacter enzymogenes* OH11 and *Saccharomyces cerevisiae*. **(A, B)** Toxic effect of four FliI-controlled secreted proteins in *Saccharomyces cerevisiae* W303 and *Escherichia coli* DH5α. **(A)** Growth of *S. cerevisiae* W303 derivative strains harboring four individual *L. enzymogenes* OH11 (OH11) genes integrated into the chromosome on non-induced (glucose) and induced (galactose) media. **(B)** Growth of *E. coli* DH5α derivative strains carrying plasmids with four individual OH11 genes on non-induced (without arabinose) and induced (with arabinose) media. In both assays, the T3SS effector protein AvrRxo1 from *Xanthomonas oryzae* pv. *oryzicola* BLS256 with known anti-bacterial and -fungal activities, was chosen as a positive control, while empty vectors were selected as negative controls. The assays were repeated three times with similar results. **(C)** Interaction between wild-type OH11 and its derivatives with *S. cerevisiae* AH109, a LacZ-labelled strain displaying a blue color in the presence of X-gal. Absence of a blue color indicated the death of *S. cerevisiae* AH109 cells. The ratios of the co-cultures wild-type OH11/*S. cerevisiae* AH109 and two FT3SS-deficient mutants (Δ*fliI* and Δ*flhB*)/*S. cerevisiae* AH109 are indicated on the top. *flhB*, a predicted FT3SS structural gene. The photograph was taken 48 h after co-inoculation. Each treatment included three biological replicates and experiments were repeated three times. (For interpretation of the references to color in this figure legend, the reader is referred to the web version of this article.)

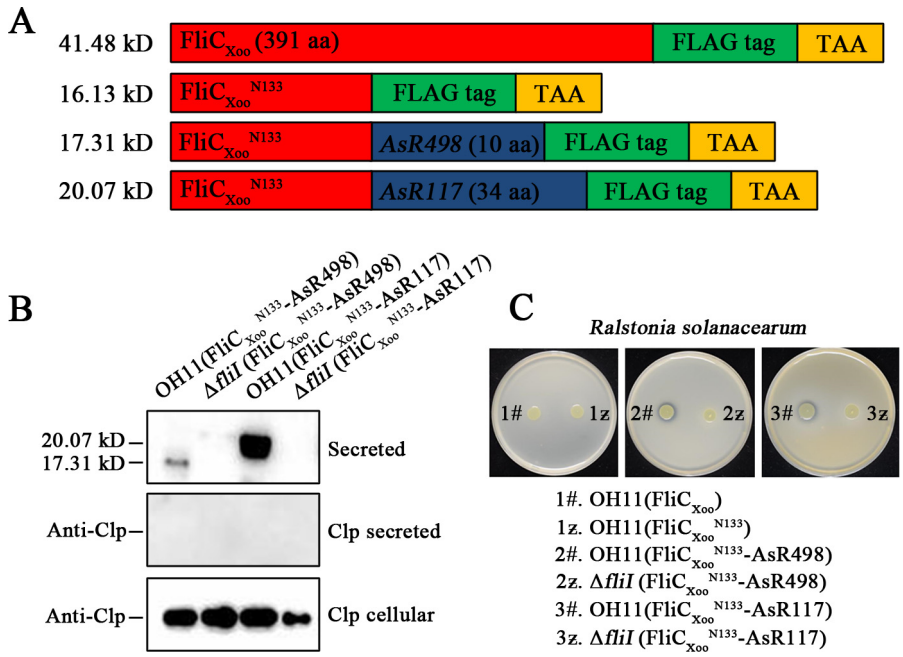

Fig. 4. The export of heterologous antibacterial toxins via the FT3SS-like system in *Lysobacter enzymogens* OH11. **(A)** Schematic maps of the recombinant constructs comprising the N-terminal signal segment of the flagellin $FliC_{Xoo}$ from *Xanthomonas oryzae* pv. *oryzae* PX099A and synthetic antibacterial peptides (AsR498 and AsR117). **(B)** Western blotting analysis of the recombinant antibacterial toxins, $FliC_{Xoo}^{N133}$-AsR498-Flag and $FliC_{Xoo}^{N133}$-AsR417-Flag in the wild-type OH11 and the Δ*fliI* mutant. Signal of each fusion protein was detected in the culture supernatant of the wild-type OH11, but not of the Δ*fliI* mutant. The cytoplasmic transcription factor Clp (25 kDa) was chosen as a loading control. **(C)** Effect of the recombinant antibacterial toxins on the *L. enzymogenes* wild-type OH11 and Δ*fliI* strain in inhibition of the *Ralstonia solanacearum* GMI1000 growth. The *R.solanacearum* GMI1000 culture was mixed with the NB agar, followed by surface inoculation of *L. enzymogenes* strains with details described in *materials and methods*. The inhibition zone (antibacterial activity) surrounding the developed macrocolonies was monitored after 36 h incubation at 28 °C.

of a potential contact-dependent competition between *L. enzymogenes* and *S. cerevisiae*. Due to the architectural similarity between FT3SS and the virulence-associated T3SS [5], we might assume that the FT3SS-like system in the non-flagellated OH11 likely adapted

to mediated microbial antagonistic interaction, a possible example of the evolution of the flagellum towards a potential injectisome involved in *L. enzymogenes* micro-predatory behavior. Taken together, the new findings of the FT3SS-mediated secretion of the native flagellar proteins and antifungal toxins in OH11 enabled us to utilize this system to export heterologous antibacterial toxins, thereby allowing OH11 to kill nearby bacterial pathogens. Through such a strategy, one could reasonably broaden the biocontrol spectrum of OH11 in crop protection, allowing it to fight against both fungal and bacterial pathogens of crops.

5. Conclusions

FT3SS is widely employed by flagellated bacteria to transport flagellar subunit proteins for flagellum assembly *in vivo*. *L. enzymogenes* is a Gram-negative soil bacterium with antifungal activities against numerous crop fungal pathogens. Intriguingly, although *L. enzymogenes* does not possess surface-attached flagellum, the genome of the model strain OH11 contains many FT3SS homologous genes. The reason for this unique phenomenon is unclear. Here, we report that the non-flagellated OH11 employs its remaining FT3SS to mediate the export of antifungal toxins. Such a functional divergence facilitates the non-flagellated OH11 to inhibit the growth of fungi, strengthening its predatory capacity. These results suggest that FT3SS more likely undergoes functional divergence in OH11, enabling an adaptive predation of fungi.

Declaration of Competing Interest

The authors declare that they have no known competing financial interests or personal relationships that could have appeared to influence the work reported in this paper.

Acknowledgments

We thank professor Zhao-Qing Luo (Purdue University, USA) for providing yeast cells and plasmids as grift. We thank Prof. You-Liang Peng (China Agricultural University, China) for helpful and insightful discussions. This research was funded by the Natural Science Foundation of Jiangsu Province (BK20190026; BK20181325), the National Natural Science Foundation of China (31872016, 32070139), the Fundamental Research Funds for the Central Universities (KJJQ202001; KYT201805 and KYTZ201403), Jiangsu Agricultural Sciences and Technology Innovation Fund [CX(18)1003] and Innovation Team Program for Jiangsu Universities (2017) and JSPS KAKENHI Grant Number JP19H03182 (to T. M.). The funders have no role in study design, data collection, data analysis, data interpretation or writing.

Author contributions

G.Q. conceived the project with input from all authors. G.Q., and F.A. designed experiments. F.A., D.S., E.Z., and X.S. performed experiments. D.S. performed the bioinformatics analysis. G.Q., D.S., X.S., and F.A. analyzed data. F.A., S.C., T.M., G.P., and G.Q wrote the manuscript. G.Q supervised the project.

Appendix A. Supplementary data

Supplementary data to this article can be found online at https://doi.org/10.1016/j.csbj.2020.10.029.

References

[1] Macnab RM. How bacteria assemble flagella. Annu Rev Microbiol 2003;57 (1):77–100. https://doi.org/10.1146/annurev.micro.57.030502.090832.
[2] Haiko J, Westerlund-Wikström B. The role of the bacterial flagellum in adhesion and virulence. Biology 2013; 2:1242–1267.
[3] Gu H. Role of Flagella in the Pathogenesis of *Helicobacter pylori*. Curr Microbiol 2017;74(7):863–9. https://doi.org/10.1007/s00284-017-1256-4.
[4] Nakamura S, Minamino T. Flagella-driven motility of bacteria. Biomolecules 2019;9:279.
[5] Minamino T, Namba K. Distinct roles of the FliI ATPase and proton motive force in bacterial flagellar protein export. Nature 2008;451(7177):485–8. https://doi.org/10.1038/nature06449.
[6] Fan F, Macnab RM. Enzymatic characterization of FliI: an ATPase involved in flagellar assembly in *salmonella typhimurium*. J Biol Chem 1996;271 (50):31981–8. https://doi.org/10.1074/jbc.271.50.31981.
[7] Minamino T, Morimoto YV, Hara N, Namba K. An energy transduction mechanism used in bacterial type III protein export. Nat Commun 2011;2:475.
[8] Morimoto YV, Kami-ike N, Miyata T, Kawamoto A, Kato T, et al. High-resolution pH imaging of living bacterial cell to detect local pH differences. mBio 2016;7: e01911–e1916.
[9] Toft C, Fares MA. The evolution of the flagellar assembly pathway in endosymbiotic bacterial genomes. Mol Biol Evol 2008;25:2069–2076.
[10] Puopolo G, Tomada S, Pertot I. The impact of the omics era on the knowledge and use of *Lysobacter* species to control phytopathogenic micro-organisms. J Appl Microbiol 2018;124(1):15–27. https://doi.org/10.1111/jam.13607.
[11] Christensen P, Cook FD. *Lysobacter*, a new genus of nonfruiting, gliding bacteria with a high base ratio. Int J Syst Bacteriol 1978;28(3):367–93. https://doi.org/10.1099/00207713-28-3-367.
[12] Li S, Du L, Yuen G, Harris SD. Distinct ceramide synthases regulate polarized growth in the filamentous fungus *Aspergillus nidulans*. MBoC 2006;17 (3):1218–27. https://doi.org/10.1091/mbc.e05-06-0533.
[13] Yu F, Zaleta-Rivera K, Zhu X, Huffman J, Millet JC, Harris SD, Yuen G, Li X-C, Du L. Structure and Biosynthesis of Heat-Stable Antifungal Factor (HSAF), a Broad-Spectrum Antimycotic with a Novel Mode of Action. AAC 2007;51(1):64–72. https://doi.org/10.1128/AAC.00931-06.
[14] Qian G, Hu B, Jiang Y, Liu F. Identification and characterization of *Lysobacter enzymogenes* a biological control agent against some fungal pathogens. Agr Sci China 2009;8:68–75.
[15] Fulano AM, Shen D, Kinoshita M, Chou SH, Qian G. The homologous components of flagellar type III protein apparatus have acquired a novel function to control twitching motility in a non-flagellated biocontrol bacterium. Biomolecules 2020;10:733.
[16] Tomada S, Puopolo G, Perazzolli M, Musetti R, Loi N, et al. Pea Broth enhances the biocontrol efficacy of Lysobacter capsici AZ78 by triggering cell motility associated with biogenesis of type IV pilus. Front Microbiol 2016;7:1136.
[17] Xia J, Chen J, Chen Y, Qian G, Liu F. Type IV pilus biogenesis genes and their roles in biofilm formation in the biological control agent *Lysobacter enzymogenes* OH11. Appl Microbiol Biotechnol 2018;102(2):833–46. https://doi.org/10.1007/s00253-017-8619-4.
[18] Qian G, Xu F, Venturi V, Du L, Liu F. Roles of a Solo LuxR in the Biological Control Agent *Lysobacter enzymogenes* Strain OH11. Phytopathology® 2014;104(3):224–31. https://doi.org/10.1094/PHYTO-07-13-0188-R.
[19] Xu G, Han S, Huo C, Chin KH, Chou SH, et al. Signaling specificity in the c-di-GMP-dependent network regulating antibiotic synthesis in Lysobacter. Nucleic Acids Res 2018; 46:9276–928.
[20] Yoshida Y, Miki T, Ono S, Haneda T, Ito M, et al. Functional characterization of the type III secretion ATPase SsaN encoded by Salmonella pathogenicity island 2. PLoS One 2014;9:e94347.
[21] Green CA, Kamble NS, Court EK, Bryant OJ, Hicks MG, Lennon C, Fraser GM, Wright PC, Stafford GP. Engineering the flagellar type III secretion system: improving capacity for secretion of recombinant protein. Microb Cell Fact 2019;18(1). https://doi.org/10.1186/s12934-019-1058-4.
[22] Munkvold KR, Martin ME, Bronstein PA, Collmer A. A Survey of the *Pseudomonas syringae* pv. *tomato* DC3000 Type III Secretion System Effector Repertoire Reveals Several Effectors That Are Deleterious When Expressed in Saccharomyces cerevisiae. MPMI 2008;21(4):490–502. https://doi.org/10.1094/MPMI-21-4-0490.
[23] Salomon D, Dar D, Sreeramulu S, Sessa G. Expression of Xanthomonas campestris pv. *vesicatoria* Type III Effectors in Yeast Affects Cell Growth and Viability. MPMI 2011;24(3):305–14. https://doi.org/10.1094/MPMI-09-10-0196.
[24] Liu Y, Zhu W, Tan Y, Nakayasu ES, Staiger CJ, et al. A Legionella effector disrupts host cytoskeletal structure by cleaving actin. PLoS Pathog 2017;13:e1006186.
[25] Kapitein N, Bönemann G, Pietrosiuk A, Seyffer F, Hausser I, Locker JK, Mogk A. ClpV recycles VipA/VipB tubules and prevents non-productive tubule formation to ensure efficient type VI protein secretion: Function of the AAA+ protein ClpV in type VI protein secretion. Mol Microbiol 2013;87(5):1013–28. https://doi.org/10.1111/mmi.12147.
[26] Triplett LR, Shidore T, Long J, Miao J. Wu S, et al. AvrRxo1 is a bifunctional type III secreted effector and toxin-antitoxin system component with homologs in diverse environmental contexts. PLoS One 2016;11:e0158856.
[27] Dobó József, Varga János, Sajó Ráchel, Végh BM, Gál Péter, Závodszky Péter, Vonderviszt F. Application of a Short, Disordered N-Terminal Flagellin Segment, a Fully Functional Flagellar Type III Export Signal, to Expression of Secreted Proteins. AEM 2010;76(3):891–9. https://doi.org/10.1128/AEM.00858-09.
[28] Burdette LA, Leach SA, Wong HT, Tullman-Ercek D. Developing Gram-negative bacteria for the secretion of heterologous proteins. Microb Cell Fact 2018;17 (1). https://doi.org/10.1186/s12934-018-1041-5.

[29] Kong Xi, Yang M, Abbas HMK, Wu J, Li M, Dong W. Antimicrobial genes from *Allium sativum* and *Pinellia ternata* revealed by a *Bacillus subtilis* expression system. Sci Rep 2018;8(1). https://doi.org/10.1038/s41598-018-32852-x.
[30] de Bruijn I, Cheng Xu, de Jager V, Expósito RG, Watrous J, Patel N, Postma J, Dorrestein PC, Kobayashi D, Raaijmakers JM. Comparative genomics and metabolic profiling of the genus *Lysobacter*. BMC Genomics 2015;16(1). https://doi.org/10.1186/s12864-015-2191-z.
[31] Hayashi F, Smith KD, Ozinsky A, Hawn TR, Yi EC, Goodlett DR, Eng JK, Akira S, Underhill DM, Aderem A. The innate immune response to bacterial flagellin is mediated by Toll-like receptor 5. Nature 2001;410(6832):1099–103. https://doi.org/10.1038/35074106.
[32] Ren T, Zamboni DS, Roy CR, Dietrich WF, Vance RE. Flagellin-deficient Legionella mutants evade caspase-1- and Naip5-mediated macrophage immunity. PLoS Pathog 2006;2:e18.
[33] Minamino T, Macnab RM. Components of the *Salmonella* Flagellar Export Apparatus and Classification of Export Substrates. J Bacteriol 1999;181(5):1388–94. https://doi.org/10.1128/JB.181.5.1388-1394.1999.
[34] Bhattacharya S, Baidya AK, Pal RR, Mamou G, Gatt YE, Margalit H, Rosenshine I, Ben-Yehuda S. A ubiquitous platform for bacterial nanotube biogenesis. Cell Rep 2019;27(2):334–342.e10. https://doi.org/10.1016/j.celrep.2019.02.055.
[35] Wu DC, Zamorano-Sánchez D, Pagliai FA, Park JH, Floyd KA, et al. Reciprocal c-di-GMP signaling: Incomplete flagellum biogenesis triggers c-di-GMP signaling pathways that promote biofilm formation. PLoS Genet 2020;16:e1008703.
[36] Hachani A, Wood TE, Filloux A. Type VI secretion and anti-host effectors. Curr Opin Microbiol 2016;29:81–93. https://doi.org/10.1016/j.mib.2015.11.006.
[37] Trunk K, Peltier J, Liu Y-C, Dill BD, Walker L, Gow NAR, Stark MJR, Quinn J, Strahl H, Trost M, Coulthurst SJ. The type VI secretion system deploys antifungal effectors against microbial competitors. Nat Microbiol 2018;3(8):920–31. https://doi.org/10.1038/s41564-018-0191-x.
[38] Bayer-Santos E, Cenens W, Matsuyama BY, Oka GU, Di Sessa G, et al. The opportunistic pathogen Stenotrophomonas maltophilia utilizes a type IV secretion system for inter bacterial killing. PLoS Pathog 2019;15:e1007651.